

Optimal Seam Line Detection in Laplacian Pyramid Domain for Image Stitching



Wu-Xia Yan^{1,2}, Chuan-Cai Liu^{1*}, Jun Hu¹

¹ School of Computer Science and Engineering, Nanjing University of Science and Technology, Nanjing 210094, PRC

² Fujian Provincial Key Laboratory of Information Processing and Intelligent Control, Minjiang University, Fuzhou 350121, PRC

wxyan127@outlook.com, chcailiu@163.com, junh_cs@126.com

Received 16 October 2016; Revised 6 March 2017; Accepted 30 March 2017

Abstract. Parallax handling is a challenging problem for image stitching. Optimal seam line method is employed in this paper to deal with the misalignment on panoramas caused by parallax problem. It's an important method for orthoimage stitching in remote sensing. However, failures occur when it used in common image stitching due to the parallax problem. In order to obtain a better panorama for common image, the proposed approach mainly employs optimal seam line and contains the following three steps. First, the parallax problem can be alleviated by geometric correction. Then, the optimal seam line is detected within the overlapping region by dynamic programming in Laplacian pyramid domain. And images were blended by using blending trick on each corresponding level of the pyramids. Finally, the convincing panorama can be obtained by reconstructing the panoramic pyramid. The experiments demonstrated that the proposed method can obtain the clear and seamless panoramas.

Keywords: image stitching, Laplacian pyramid, remote sensing, seam line

1 Introduction

Image stitching under different conditions is at the core of variety of applications, including remote sensing, medical image analysis, photogrammetry, video processing, computer graphics and computer vision [1]. Technical background for image stitching can be found in work by Szeliski [2]. The problem of image stitching can be turned into transformation problem between images with overlapping regions in general [3]. Accordingly, the classical projective transformation is related by homography [4]. However, homographies are justified only if the camera movement is a strictly pure rotation, or the imaged scene is effectively planar (i.e., when the scene is sufficiently far away from the camera) [5]. This assumption guarantees that there is no or little parallax on input images. When the underlying assumptions are not met, artifacts like ghosting, shadow, or broken image structures appear on panoramas. More specifically, the case without this assumption can be successful when the transformation surface is cylindrical, spherical or cubic, rather than a planar. But the requirement of knowing the focal length and the tilting angle of the camera cannot be easily met in practical applications.

To deal with the problem of parallax, the projective transformation method has turned into locally non-rigid models in more recent works. Such as the dual-homography warping [6], it got different transformation matrices for different local regions. The smoothly varying affine (SVA) warp [7] adopts multiple local warps on the overlapping regions to account for misalignment. The as-projective-as-possible (APAP) warp [8] aims to be globally projective while allowing locally non-projective deviations to account for parallax. Chang [9] proposed the shape preserving half projective (SPHP) warp. It combined a projective transformation and a similarity transformation. For the non-overlapping regions,

* Corresponding Author

projective transformation is used for smoothly extrapolating warps beyond the image overlap and resembling a global transformation on the global image. Zhang [10] proposed a parallax tolerant image stitching method, which can only align images on the local region. However, it requires the scene content can be modeled by two planes. For the large-scale stitching problem, Xia [11] proposed a generic framework for globally consistent alignment of images captured from approximately planar scenes via topology analysis. It can resist the perspective distortion meanwhile preserving the local alignment accuracy. Pun [12] proposed a local matching method to establish the region correspondence by segmenting the image into closed regions firstly. However, all of the above works are either time consuming or can only work well with some sparse sets of input images which met the underlying assumption. They still cannot handle images with large parallax.

However, orthoimage stitching using the seam line technique can obtain satisfactory panoramas without such constraints on the input images. It also has a significant impact on the final panoramic image quality [13]. Meanwhile, seam line technique has become an active research topic in the fields of remote sensing, digital imagery and orthophotography. For example, a good survey can be found in work proposed by Soille [14]. This approach has created a lot of excitement in orthoimage stitching. One of the first published algorithms of seam line detection is proposed by Milgram [15], where the pixels of seam line defined as the pixels that minimizing the sum of gray level difference in the overlapping region. The enhanced approach that suggested by the same author considered the seam line as a least cost path. Afek et al. [16] detected the seam line through marginal zone triangulation on the tie points. Fernandez et al. [17] defined the seam line by bottleneck shortest paths. The seam line searching process was further modeled by a Greedy Randomized Adaptive Search Procedure (GRASP) [18]. Moreover, representative work [19] introduced the energy function of the snake (i.e., the active contour model) for detecting the optimal seam line.

Comparing with currently existing methods, image stitching using seam line technique is quite a different way. Instead of acquiring homography from the matched points, the seam line method needs to acquire a curve consisted by pixels in the overlapping region. Furthermore, the original information of the input images can be preserved while the projective distortions on the panoramas can be avoided. These advantages of the seam line technique inspired our work. That is, common images even with parallax can acquire convincing panoramas by seam line technique.

Seam line on the energy map consisted by pixels with the maximum similarity of image colour, intensity, edge and so on [20]. However, it has a major difference for searching seam line between orthoimage and common image. The detection scope of orthoimage is the entire image. Nevertheless, the relationship between common images can only exist in the overlapping region. On the other hand, the integrity of objects (e.g., building, road or forest) in orthoimages must be maintained [21]. Hence seam line should not cut across objects. However, there is no such restriction for common image.

Inspired by these observations, we employ the optimal seam line method to obtain a better panorama (without ghosting, shadow or other artifacts) for common image stitching. The key contributions of our work are presented here:

(1) The idea of using optimal seam line as a natural and simple way to stitch common images is exploited. We detect the optimal seam line in the gradient domain rather than in the intensity domain.

(2) The parallax problem can be alleviated by geometric correction in the first place. Besides, interpolation artifacts can be avoided by using a blending trick in this paper. Furthermore, the panorama was smoothed by reconstructing all the panoramic layers during image blending.

2 Geometric Rectification

Without loss of generality, image stitching is represented as a collection of images with associated geometrical transformation. In general, input images with different image coordinates have different image geometric spaces, which result in the parallax. Hence, we first unify the coordinate of input image pair with geometric correction. Specifically, let I_0 and I_1 be the image pair with overlapping regions (I_0 is the reference image). Homography H_{01} which assigned to this corresponding image points ($X_0 = (x_0, y_0, 1)^T$ and $X_1 = (x_1, y_1, 1)^T$) is defined as below.

$$X_1 = H_{01}X_0. \quad (1)$$

$$\begin{bmatrix} x_1 \\ y_1 \\ 1 \end{bmatrix} = \begin{bmatrix} h_0 & h_1 & h_2 \\ h_3 & h_4 & h_5 \\ h_6 & h_7 & h_8 \end{bmatrix} \begin{bmatrix} x_0 \\ y_0 \\ 1 \end{bmatrix}. \quad (2)$$

where $H_{01} \in R^{3 \times 3}$ is homogeneous matrix. Without loss of generality, we set $h_8 = 1$. Then, Eq. (2) can be rewritten as follow:

$$\begin{cases} x_1 = \frac{h_0 x_0 + h_1 y_0 + h_2}{h_6 x_0 + h_7 y_0 + 1} \\ y_1 = \frac{h_3 x_0 + h_4 y_0 + h_5}{h_6 x_0 + h_7 y_0 + 1} \end{cases}. \quad (3)$$

From Eq. (2), we can see that the projective transformation H_{01} has eight degrees of freedom. Since each point correspondence provides two equations (i.e. Eq. (3)), four correspondences are sufficient to compute H_{01} with the restriction that there is no three points be collinear [22]. We extracted SIFT features and matched them by KNN. Outliers are removed by RANSAC. Then we can get H_{01} . Meanwhile, the image pairs can be rectified into the same image geometric space (i.e. coordinate system) as the reference image. The parallax problem can be alleviated.

3 Optimal Seam Line Detection

A seam line is a path of pixels detected from each row or column of image, which is either vertical or horizontal. Let I_0, I_1 be two input images for a stitching algorithm. Assumes there is a pixel curve $\hat{y} = f(\hat{x})$. The difference of pixels between the two sides of the curve should be minimal:

$$I_s = \begin{cases} I_0(x, y) & x < \hat{x} \\ I_1(x, y) & x \geq \hat{x} \end{cases}. \quad (4)$$

From Eq. (4), we must determine which pixel belongs to the optimal seam line in the overlapping region. Furthermore, the importance of a pixel is measured by contrasting with its neighboring pixels on the energy map. The energy map will be introduced in the Laplacian pyramid domain as below.

3.1 Energy Map in the Laplacian Pyramid Domain

The Laplacian pyramid is ubiquitous for decomposing images into multiple scales. More concretely, as shown in Fig. 1, the Gaussian pyramid (G_3, G_2, G_1, G_0) of the leftmost part constructs the low pass bands. The Laplacian layers (L_3, L_2, L_1, L_0) are constructed by the details that distinguish successive levels of the Gaussian pyramid (bandpass images). The rightmost part of Fig. 1 is the procedure of pyramid reconstruction conversely. Accordingly, during the transformation from one image into its Laplacian pyramid domain, the input image is successively decomposed into approximate Gaussian layers. The sequence with different values of low pass bands under an expanded function is termed Laplacian layers. Hence the bandpass images contain the residual information, which represents edges or other detailed image features. In this paper, each of the Laplacian pyramid layer within the overlapping region scope is considered as an energy map.

3.2 Seam Line Detection and Quality Assessments

Dynamic programming (DP) is a programming method that stores the results of sub-calculations. It is used here to detect the optimal seam line. Given an image and the pixel point $x(i, j)$ of this image, the energy function $L(i, j)$ of the optimal seam line is as follow:

$$L(i, j) = \begin{cases} \infty, & \text{if } j < 1 \\ x(i-1, j), & \text{if } i = 1. \\ \min(L(i-1, j-1), L(i-1, j), L(i-1, j+1) + x(i, j)), & \text{other} \end{cases} \quad (5)$$

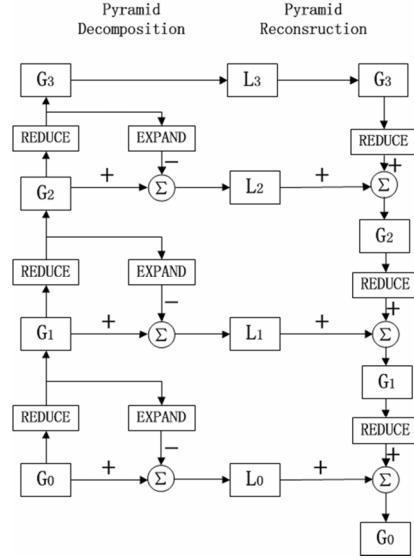


Fig. 1. The Laplacian pyramid algorithm

First, initialize all the pixels on the first line of the image overlapping region as the first pixels of the optimal seam lines. Then, traverse this image from the second row to the last row and compute all the cumulative minimum energy L for any possible connected pixels. Finally, the line with the minimum value of L is chosen as the optimal seam line. The definition of L for horizontal seam line is similar.

On the other hand, the seam line quality assessment [23] is defined as an error measurement:

$$E(p) = \min_{R \in I_1, I_2} \|P - R\|^2. \tag{6}$$

where p represents each pixel of the seam line. We estimate the error value $E(p)$ by extracting a 10×10 patch P , which centered at p . R represents all image patches in the overlapping region of I_1 and I_2 .

From Eq. (6), we can search the most similar patch of $E(p)$ in the overlapping region of images I_1 and I_2 . Then, the seam line with the highest quality is chosen as the optimal seam line. We compared the quality of seam lines detected from different domains on different images (shown in Fig. 2) and listed the results in Table 1. Let S_1 be seam lines detected in the gradient domain by our method. S_2 represents the seam lines detected by the same image stitching method without geometry correction. S_3 represents the seam lines which detected in the intensity domain. We can see that seam lines S_1 detected by our proposed method are the optimal seam lines.

Table 1. Error metric of seam lines obtained by different methods

$E(p)$	$Building_1$	$Building_2$	$Building_3$	$Building_4$
S_1	$3.306 e^{-4}$	$6.281 e^{-4}$	$1.846 e^{-4}$	$2.2072 e^{-4}$
S_2	$7.648 e^{-3}$	$7.865 e^{-3}$	$9.452 e^{-3}$	$3.791 e^{-3}$
S_3	$3.821 e^{-3}$	$4.283 e^{-3}$	$2.829 e^{-3}$	$1.253 e^{-3}$

4 Image Blending

Here a blending trick [24] was given. It started with an empty panoramic canvas. As shown in Fig. 2, I_0 and I_1 are segmented by the optimal seam line. I_0 is the reference image. Then the left part of I_0 (Fig. 2(b)) and the right part of I_1 (Fig. 2(c)) are composite on the panoramic canvas to obtain the final panoramic image (Fig. 2(a)).

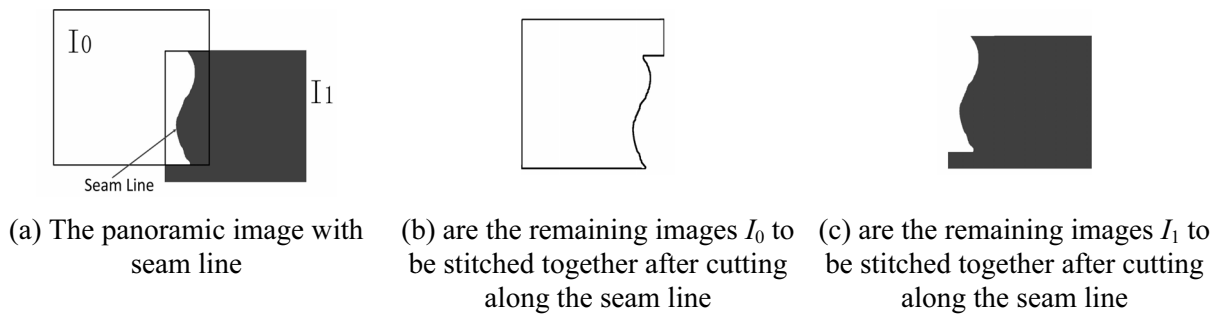


Fig. 2. The image blending process (I_0 is the reference image)

We got Laplacian pyramid levels for each image first. According to the experimental results, we chose three Laplacian pyramid levels for each input image. Secondly, the optimal seam line was detected on each corresponding level. Then, the same level of the corresponding Laplacian pyramid was blended by the above mentioned blending trick to obtain one panoramic pyramid layer. Finally, the composite panorama reconstructed by collapsing all the panoramic pyramid layers. As image blending happened on each Laplacian pyramid level, the artifacts along the optimal seam line are smoothed. The clear and seamless panorama can be obtained.

When overlapping area is from more than two input images, the detection of the optimal seam line is complex. Input images are processed one by one in sequence. Accordingly, the reference image is updated with the stitched image acquiring from the previous step. We repeat these steps until all the input images are processed.

Algorithm of this paper is outlined as below:

```

Algorithm1 {Image Stitching by Optimal Seam Line Detection in
Laplacian Pyramid Domain};
begin
  Choose the reference image  $I_r$  (the rest images are  $I_m$ );
  Set  $i := 0$ ;
  while  $I_m \neq null$  do
    Get the image  $I_i$  from  $I_m$  which has overlapping region with  $I_r$ ;
    Do geometric correction and build Laplacian pyramid for image  $I_m$ 
    and  $I_r$ ;
    for each corresponding pyramid level of  $I_m$  and  $I_r$  do
      Find the optimal seam line by DP in the overlapping region;
      Blend the corresponding levels along the seam line to obtain one
      panoramic pyramid level;
    end for.
    Reconstruct the panorama of  $I_m$  and  $I_r$  by collapsing all the
    panoramic pyramid layers;
    Update the reference image  $I_r$  with  $I_s$ ;
    Set  $i := i + 1$ ;
  end while.
  return  $I_s$ ;
end.

```

5 Experiment Results and Analysis

The input images for our experiments are captured from different camera positions. They consist of three groups of two input images, two groups of three input images and one group of six input images. All the experiments were performed on a PC with 2GB of RAM and a 2.93 GHz Intel CPU.

We compared results of different image stitching methods. To explain the importance of geometric correction, we give the results by the proposed method M_1 and results of the same image stitching method without geometric correction M_2 . Then, in order to compare the quality of seam lines detected in

different domains, we give results of method M_3 , from which the seam line detected in the intensity domain. Meanwhile, we also compare the traditional projective transformation M_4 , APAP warps M_5 [8] and SPHP warps M_6 [9]. All the experimental results are shown in Fig. 3.

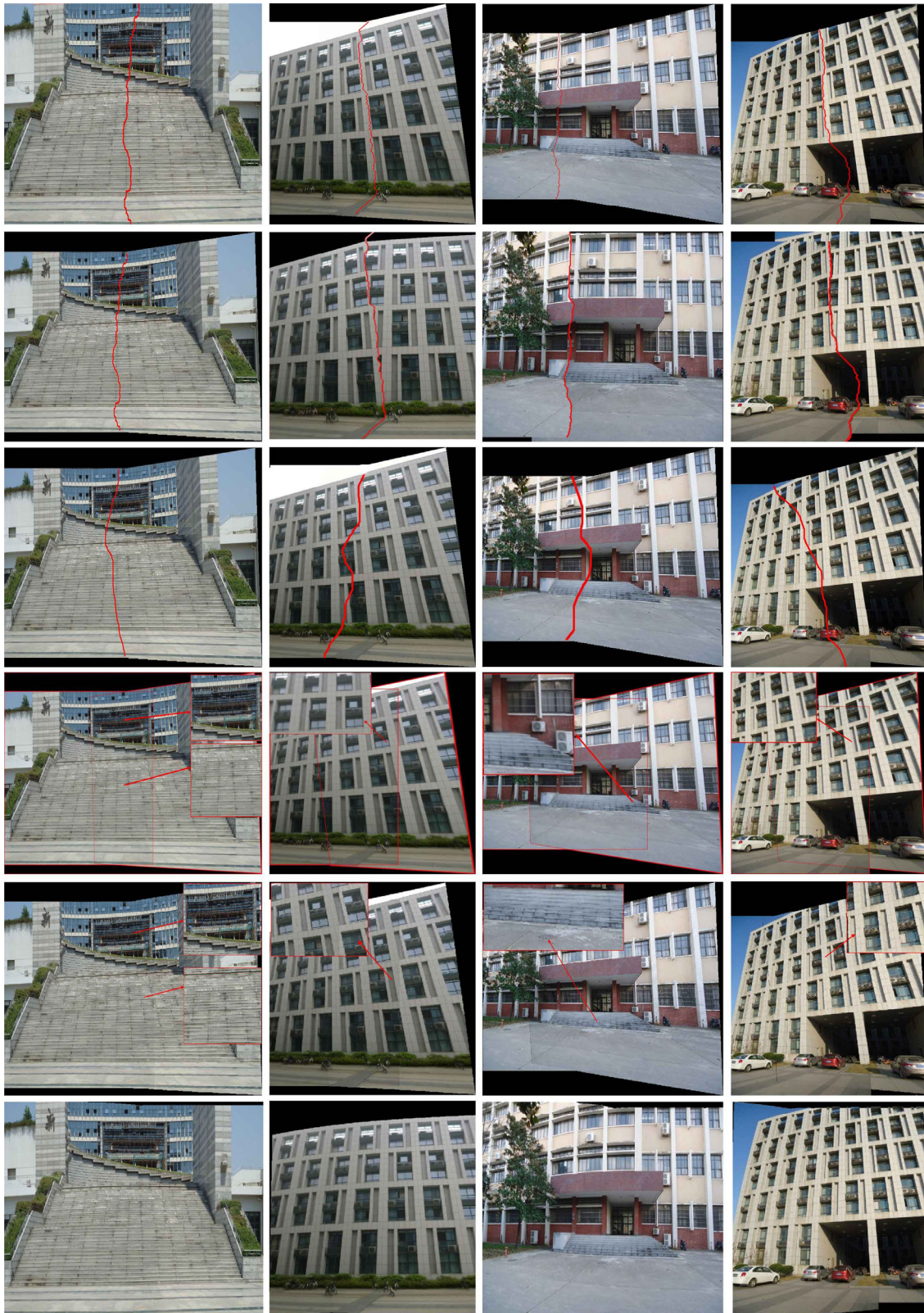
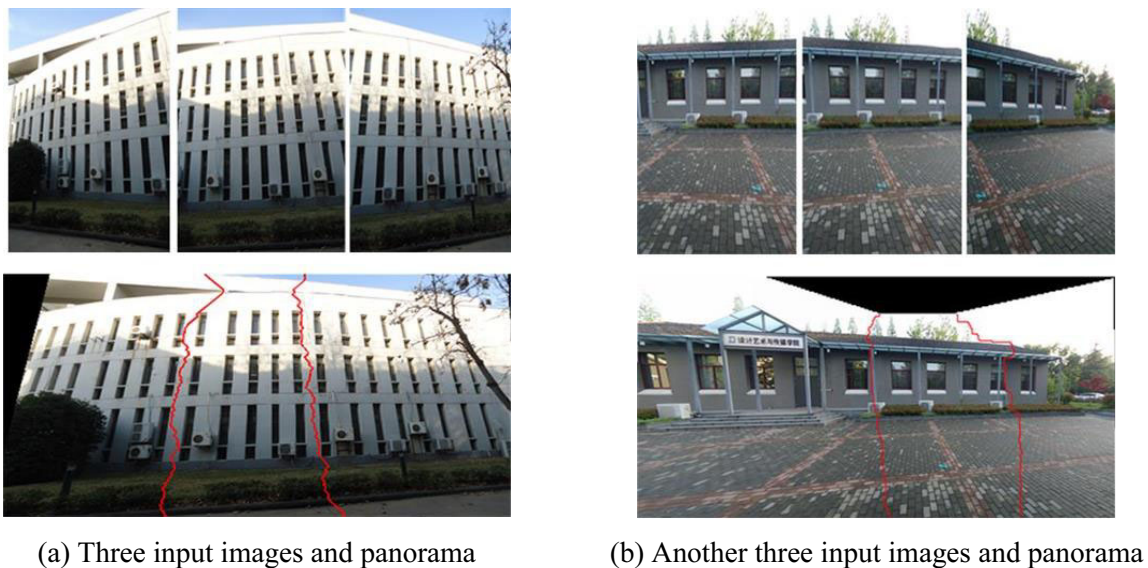


Fig. 3. Panoramas are acquired by different image stitching methods

From Fig. 3, we can see that the first row results from M_1 seem smoother and more natural than the second row from M_2 . This is because the input images with parallax have different image geometric spaces. They cannot be pasted together by the seam line without preprocessing directly, or it will result in broken structures along the seam line.

The third row acquired from M_3 seems the same good as the results acquired by M_1 . However, from Table 2 we can see that the quality of seam lines acquired by M_1 is much better. Moreover, the fourth row from M_4 with boundaries of each input image has been highlighted in red color. The overlapping region is easily to be identified. The close-ups show stitching details. The results are marginally better than our method. But significant ghost remains on each panorama. The fifth row from M_5 also shows many blur areas and shadows in the overlapping regions. The twisted effect is obvious in the overlapping region on the last row from M_6 . Because of this method is a combination of a projective transformation and a similarity transformation. The transitional region still needs post-processing. Clearly, the clearest and smoothest panoramas are obtained by the proposed method M_1 .

To test the performance of the proposed method again, results of stitching three input images are shown in Fig. 4. The middle of the image is chosen as the reference image.



(a) Three input images and panorama

(b) Another three input images and panorama

Fig. 4. Two groups of panoramas with three input images got by our method

Result of stitching six input images is shown in Fig. 5(f). The process includes three steps (as shown in Figs. 5(b), 5(c) and 5(d)).

The total run time information is shown in Table 2. All methods were run on MATLAB platform for warping and blending with different images size from 463×617 pixels to 619×824 pixels. In contrast, the proposed method spent the least time from all these image stitching methods.

To quantify the alignment accuracy, we compute the root mean squared error (RMSE) of a warp f on a set of key point matches $\{x_i, x'_i\}_{i=1}^N$:

$$RMSE(f) = \sqrt{\frac{1}{N} \sum_{i=1}^N \|f(x_i) - x'_i\|^2} \quad (7)$$

where $f: R^2 \mapsto R^2$. The available SIFT point matches are randomly partitioned into a training set and testing set for each image pair. The training set is used to learn a transformation, and the RMSE is evaluated over both sets.

Table 3 depicts the average errors. It is obvious that the method proposed in this paper provides the lowest errors in all of the image pairs.



Fig. 5. Panoramas with six input images got by our method

Table 2. Comparing of time consuming (s)

No.	M_1	M_2	M_3	M_4	M_5	M_6
1	2.326	3.448	3.164	2.927	7.132	3.729
2	1.340	3.414	3.963	2.625	4.283	3.921
3	2.258	2.665	2.593	3.119	5.182	5.318
4	1.347	3.927	3.628	2.216	4.837	6.927

Table 3. Average *RMSE* (in pixels, *TR* is the training set error, *TE* is the testing set error, the suffix means the number of image pair from Fig. 3)

<i>RMSE</i>	M_1	M_2	M_3	M_4	M_5	M_6
<i>TR</i> ₁	16.406	18.491	17.733	21.306	19.437	20.766
<i>TE</i> ₁	15.972	18.276	17.382	21.033	20.762	19.671
<i>TR</i> ₂	15.302	17.924	18.916	19.297	19.509	17.128
<i>TE</i> ₂	15.106	17.194	17.823	19.328	19.002	18.081
<i>TR</i> ₃	12.873	16.092	16.163	18.194	16.217	14.987
<i>TE</i> ₃	12.882	16.249	17.637	18.023	15.096	15.829
<i>TR</i> ₄	10.664	12.635	14.829	15.745	14.271	13.312
<i>TE</i> ₄	10.423	12.433	13.616	15.284	14.291	14.829

6 Conclusions

A novel optimal seam line method for common image stitching has been proposed in this paper. Since the panoramas of common images are often accompanied by ghost or other artifacts. We can get clear and seamless panoramas in three steps. We alleviate the parallax problem with geometric correction first. Then, the blending trick was employed to avoid projective distortions. Finally, seamless panoramas for common images are acquired by reconstructing all the panoramic layers. With different groups of image stitching experiments, we have shown that the proposed method can enhance the stitching quality obviously. Our geometric rectification procedure currently does not take feature accuracy into account. Therefore, when the scene is lack of feature or textures, the projective transformation can be ineffective in reducing projective distortion. In the future, we would like to explore the possibility of adopting our method to applications such as image stitching on mobile devices. We would also like to use deep learning algorithms for extracting features [25, 26] to improve the accuracy of image alignment.

Acknowledgements

This research was supported by Open Fund Project of Fujian Provincial Key Laboratory of Information Processing and Intelligent Control (Minjiang University) (Project No. MJUKF201714).

References

- [1] Z.H. Hao, S.W. Ma, F. Zhao, Atlas compatibility transformation: A normal manifold learning algorithm, *International Journal of Automation and Computing* 12(4)(2015) 382-392.
- [2] S. Richard, Image mosaicing for tele-reality applications, in: *Proc. IEEE Workshop on Applications of Computer Vision* 1994.
- [3] C.C. Lin, S.U. Pankanti, K.N. Ramamurthy, A.Y. Aravkin, Adaptive as-natural-as-possible image stitching, in: *Proc. IEEE Conference on Computer Vision and Pattern Recognition (CVPR)*, 2015.
- [4] B. Matthew, D. G. Lowe, Automatic panoramic image stitching using invariant features, *International Journal of Computer Vision* 74(1)(2007) 59-73.
- [5] Z.L. Szapak, W. Chojnacki, A.V.D. Hengel, Robust multiple homography estimation: an ill-solved problem, in: *Proc. the*

- IEEE Conference on Computer Vision and Pattern Recognition, 2015.
- [6] J.H. Gao, S.J. Kim, M.S. Brown, Constructing image panoramas using dual-homography warping, in: Proc. IEEE Conference on Computer Vision and Pattern Recognition (CVPR), 2011.
- [7] W.Y. Lin, S. Liu, Y. Matsushita, T.T. Ng, L.F. Cheong, Smoothly varying affine stitching, in Proc. IEEE CVPR 2011, 2011.
- [8] Z. Julio, T.J. Chin, M.S. Brown, D. Suter, As-projective-as-possible image stitching with moving DLT, in Proc. the IEEE Conference on Computer Vision and Pattern Recognition, 2013.
- [9] C.H. Chang, Y. Sato, Y.Y. Chuang, Shape-preserving half-projective warps for image stitching, in: Proc. IEEE Conference on Computer Vision and Pattern Recognition, 2014.
- [10] F. Zhang, F. Liu, Parallax-tolerant image stitching, in: Proc. the IEEE Conference on Computer Vision and Pattern Recognition, 2014.
- [11] M. Xia, J. Yao, R. Xie, L. Li, W. Zhang, Globally consistent alignment for planar mosaicking via topology analysis, *Pattern Recognition* 66(C)(2017) 239-252.
- [12] C.M. Pun, C. Yan, X.C. Yuan, Image alignment-based multi-region matching for object-level tampering detection, in: Proc. IEEE Transactions on Information Forensics and Security, 2017.
- [13] T.H. Kwok, Y.Q. Zhang, C.C. Wang, Y.J. Liu, K. Tang, Styling evolution for tight-fitting garments, in: Proc. IEEE Transactions on Visualization and Computer Graphics, 2016.
- [14] P. Soille, Morphological image compositing, in: Proc. IEEE Transactions on Pattern Analysis and Machine Intelligence, 2006.
- [15] D.L. Milgram, Computer methods for creating photomosaics, in: Proc. IEEE Transactions on Computers, 1975.
- [16] Y. Afek, A. Brand, Mosaicking of orthorectified aerial images, in: Proc. Photogrammetric Engineering and Remote Sensing, 1998.
- [17] E. Fernandez, R. Garfinkel, R. Arbiol, Mosaicking of aerial photographic maps via seams defined by bottleneck shortest paths, *Operations Research* 46(3)(1998) 293-304.
- [18] E. Fernández, R. Martí, GRASP for seam drawing in mosaicking of aerial photographic maps, *Journal of Heuristics* 5(2)(1999) 181-197.
- [19] A. Levin, A. Zomet, S. Peleg, Y. Weiss, Seamless image stitching in the gradient domain, in: Proc. European Conference on Computer Vision, 2004.
- [20] J.H. Lee, K. Kim, J. Park, J.Y. Park, S.W. Jung, Image recomposition using seam carving and insertion considering the rule of thirds, *IEEE Transactions on Smart Processing and Computing* 5(1)(2014) 1-4.
- [21] J. Tian, X. Li, F. Duan, J. Wang, Y. Ou, An efficient seam elimination method for UAV images based on Wallis Dodging and Gaussian distance weight enhancement, *Sensors* 16(5)(2016) 662.
- [22] R. I. Hartley, In defense of the eight-point algorithm, *IEEE Transactions on Pattern Analysis and Machine Intelligence* 19(6)(1997) 580-593.
- [23] J. Gao, Y. Li, T. J. Chin, M. S. Brown, Seam-Driven Image Stitching, in: Proc. Eurographics, 2013.
- [24] Y. Xiong, K. Turkowski, Registration, calibration and blending in creating high quality panoramas, in: Proc. IEEE Workshop on Applications of Computer Vision, 1998.
- [25] S. Chakraborty, P.K. Patra, P. Maji, A.S. Ashour, N. Dey, Image Registration Techniques and Frameworks: A Review, in: N. Dey, A. Ashour, S. Acharjee (Eds.), *Applied Video Processing in Surveillance and Monitoring Systems*, IGI Global, Hershey, PA, 2017.

- [26] X. Gibert, V. M. Patel, R. Chellappa, Deep multitask learning for railway track inspection, IEEE Transactions on Intelligent Transportation Systems 18(2017) 153-164.